HIGH-RESOLUTION MASS SPECTROMETRY APPLIED TO THE IDENTIFICATION OF TRANSFORMATION PRODUCTS OF QUINOLONES FROM STABILITY STUDIES AND NEW METABOLITES OF ENROFLOXACIN IN CHICKEN MUSCLE TISSUES

F.J. Morales-Gutiérrez, M.P. Hermo, J. Barbosa, D. Barrón*.

Department of Analytical Chemistry. Food and Nutrition Torribera Campus. University of Barcelona.

Avda. Prat de la Riba, 171.

Sta. Coloma de Gramenet, E-08921, Barcelona, Spain.

* Correspondence to:

e-mail: dolores.barron@ub.edu

Tel: +34 93 4033797 / 21277

Fax: +34 93 4021233

Abstract

The aim of this work was the identification of new metabolites and transformation products (TPs) in chicken muscle from Enrofloxacin (ENR), Ciprofloxacin (CIP), Difloxacin (DIF) and Sarafloxacin (SAR), which are antibiotics that belong to the fluoroquinolones family. The stability of ENR, CIP, DIF and SAR standard solutions versus pH degradation process (from pH 1.5 to 8.0, simulating the pH since the drug is administered until its excretion) and freeze-thawing (F/T) cycles was tested. In addition, chicken muscle samples from medicated animals with ENR were analyzed in order to identify new metabolites and TPs.

The identification of the different metabolites and TPs was accomplished by comparison of mass spectral data from samples and blanks, using liquid chromatography coupled to quadrupole time-of-flight (LC-QqToF) and Multiple Mass Defect Filter (MMDF) technique as a pre-filter to remove most of the background noise and endogenous components. Confirmation and structure elucidation was performed by liquid chromatography coupled to linear ion trap quadrupole Orbitrap (LC-LTQ-Orbitrap), due to its mass accuracy and MS/MS capacity for elemental composition determination.

As a result, 21 TPs from ENR, 6 TPs from CIP, 14 TPs from DIF and 12 TPs from SAR were identified due to the pH shock and F/T cycles. On the other hand, 14 metabolites were identified from the medicated chicken muscle samples. Formation of CIP and SAR, from ENR and DIF, respectively, and the formation of desethylene-quinolone were the most remarkable identified compounds.

Keywords: Quinolones, chicken muscle, metabolites, transformation products, high-resolution mass spectrometry.

1. Introduction

Quinolones are one of the most widely used class of antibiotics in human and veterinary medicine. Their main uses in veterinary are therapeutic (treatment of bacterial infections), prophylactic (prevention of infections) and as growth promoters of animals intended for human consumption, although this last use is not allowed in the European Community [1,2].

Misuse of antibiotics in animals and the medicated animal slaughter before the metabolism and excretion of the antibiotic after therapeutic treatment, can lead to the presence and accumulation of residues of these antibiotics and their metabolites in food for human consumption. The intake of this food can result to health risks, such as allergy problems, toxicity and potential development of resistant bacterial strains when these antibiotic residues pass to humans through the food chain [3].

In order to regulate the use of these substances, to avoid risks to consumer health, the European Community has laid down a set of policies and measures, including the establishment of maximum residue limits (MRLs) for these antibiotics in animal food according to each species and tissue. A list of allowed substances, with MRL, is available in the Annex I of Commission Regulation 37/2010 [4,5]. However, this legislation generally include only the active compound (antibiotic) and in some cases, the main known metabolite. Other unknown metabolites and TPs possibly formed through the pH shock (from 1.2 in stomach to 8.0 in colon), interaction with biological substances or the own animal metabolism are not included in this Regulation. In addition, new TPs could be formed due to the complex sample treatment, which could be wrongly interpreted as metabolites and could contribute to pharmacological activity. Therefore, the identification of these unknown metabolites and TPs becomes necessary

to understand the possibly associated toxicity or harmful effects to human health and to avoid misleading results.

In the literature, most of the TPs and metabolites described for quinolones come mainly from photo-degradation studies in environmental samples [6-12] and microbiological transformation products [13-20]. However, to our knowledge, studies focused on metabolites and TPs as antibiotic residues in animal tissues for human consumption, generated by biotransformation processes after pharmacological treatment, are scarcely described in the literature [21-23].

Accordingly, the present study was focused on the effect of pH and F/T cycles on the formation of TPs from ENR, CIP, DIF and SAR, as well as the determination and identification of new metabolites and TPs from chicken muscle samples from medicated animals with ENR.

2. Experimental

2.1. Reagents and materials

Quinolones were purchased from different pharmaceutical firms: Enrofloxacin (ENR) from Cenavisa (Reus, Spain), Ciprofloxacin (CIP) from Ipsen Pharma (Paris, France), Difloxacin (DIF) and Sarafloxacin (SAR) from Abbot (Madrid, Spain). Quinolones were in their free form with a purity of ≥99%, according to the specifications of the pharmaceutical firms.

Hydrochloric acid (HCl), acetic acid (HAcO), formic acid (HFo), trifluoroacetic acid (TFA), diethylmalonic acid (DEMA), ammonia (NH_3), potassium dihydrogenphosphate (KH_2PO_4), sodium hydroxide (NaOH), methanol (MeOH, HPLC grade) and acetonitrile (MeCN, HPLC and MS grade) were provided from Merck (Darmstadt, Germany). Dichloroacetic acid (DCA) was provided from Carlo Erba (Milano, Italia) and ammonium acetate (NH_4AcO, MS grade) from Sigma-Aldrich (St. Louis, MO, USA).

Ultrapure water was obtained from a MilliQ system from Millipore (Billerica, MA, USA). Solid-phase extraction (SPE) cartridges Isolute ENV+ (3 mL / 200 mg) were supplied by Biotage AB (Uppsala, Sweden). The 22 and 45 µm nylon filter membranes by Sharlab (Barcelona, Spain) were used to filter the extracts before injection in the chromatographic system.

2.2. Preparation of standard and working solutions

Individual ENR, CIP, DIF and SAR stock solutions were prepared at a concentration of 100 mg L^{-1} in HAcO 0.050 mol L^{-1}.

In order to investigate the generation of TPs at different pH values, buffers between pH 1.5 and 8.0 were prepared to make the antibiotic working solutions. pH 1.5 was obtained from an aqueous solution of DCA 0.1% (v/v) and adjusted with HCl 1.0 mol L^{-}

[1]; pH 2.0 and 2.5 buffers were reached with HFo 0.1% (v/v) adjusted with HCl 1.0 mol L^{-1} and NH_3 0.1 mol L^{-1}, respectively; pH 3.0 and 3.5 buffers were obtained from HAcO 0.1% (v/v) adjusted with HCl 0.1 mol L^{-1} and NH_3 0.1 mol L^{-1}, respectively; pH 4.5 and 5.5 buffers were also obtained from HAcO 0.1% (v/v) adjusted with NH_3 1.0 mol L^{-1}. An aqueous solution of DEMA 0.010 mol L^{-1} was used for pH 6.5 and 8.0 buffers, the solution was adjusted with HCl 0.1 mol L^{-1} and NH_3 1.0 mol L^{-1}, respectively.

Phosphate solution (0.050 mol L^{-1}) was adjusted to pH 5.0 with NaOH 0.1 mol L^{-1}. Hydroorganic solution TFA:H_2O:MeCN (2:23:75, v/v/v) were also prepared.

2.3. Instrumentation

Liquid chromatography with ultraviolet detection (LC-UV) analyses were performed using an HP Agilent Technologies 1100 quaternary pump liquid chromatograph (Waldbronn, Germany).

LC-MS analyses were performed using an Agilent 1200 RRLC binary pump liquid chromatograph (Waldbronn, Germany) coupled to a hybrid quadrupole time-of-flight QSTAR Elite Mass Spectrometer from Applied Biosystems (Concord, Ontario, Canada), equipped with a Turbo Ion Spray source.

Both LC separations were carried out using an Agilent Zorbax Eclipse XDB-C_8 column of 150 x 4.6 mm i.d. 5µm (Waldbronn, Germany) protected by a Kromasil C_8 20 x 4.5 mm i.d. 5µm guard column from Aplicaciones Analíticas (Barcelona, Spain), working at room temperature.

LC-MS/MS analyses were performed using an Accela HPLC system from Thermo Fisher Scientific (Hemel Hempstead, UK) coupled to a linear ion trap quadrupole-Orbitrap (LTQ-Orbitrap) Velos-Hybrid FT Mass Spectrometer from Thermo Fisher Scientific (Hemel Hempstead, UK), equipped with a heated electrospray ionization

(HESI) interface. The LC separation was carried out using a Waters Simmetry C_8 50 x 2.1 mm i.d. 5µm (Milford, Massachusetts, USA), working at room temperature.

SPE was carried out on a SUPELCO vacuum manifold connected to a SUPELCO vacuum tank (Bellefone, PA, USA).

Auxiliary apparatuses were: a CRISON 2002 potentiometer (±0.1 mV) (Barcelona, Spain) equipped with a CRISON 5203 combined pH electrode from Orion Research (Boston, MA, USA) used to measure the pH of the buffer solutions; a centrifuge 460R of Hettich Zentrifugen (Tuttlingen, Germany) used in sample treatment and a TurboVap LV system from Caliper LifeSciences (Hopkinton, MA, USA) with nitrogen stream for the evaporation of the extracts. An analytical balance with a precision of ±0.1 mg and a vortex-mixer were also used.

2.4. Procedures

2.4.1. Preliminary stability studies

In order to study the stability of quinolones versus pH and F/T cycles, stock solutions of each antibiotic were diluted in each buffer solution (pH values from 1.5 to 8.0) to obtain a concentration of 10 mg L^{-1} and analyzed after 1, 2 and 3 F/T cycles at -20ºC. Samples were kept at -20ºC for 24h between each F/T cycle.

In addition, blanks were prepared taking 100 µL from the 0.050 mol L^{-1} HAcO solution and were diluted in each buffer solution.

2.4.2. Medicated animal samples

Chicken muscle samples from medicated animals with ENR were analyzed. Chickens were medicated according to the pharmacological administration protocol fit for human consumption. The therapeutic treatment involved a daily dose of 16 mg/kg of ENR

dissolved in the chicken drinking water during 4 days. Fresh pre-solutions of the antibiotic and the medicated water were prepared every day just before it is offered to the animals. Two types of samples were analyzed; two male broiler chickens slaughtered on the third day of the pharmacological treatment (3-day treated) and two male broiler chickens slaughtered four days after pharmacological treatment ends (post-treatment). In addition, two male broiler chickens (non-medicated chickens) randomly selected from the poultry farm were sacrificed and used as blanks. Chickens were sacrificed after 23 days (3-day treated) and 28 days (post-treatment and blanks) of life. Meat was minced, homogenized and stored at -20ºC until sample treatment.

2.4.3. Sample preparation

Samples were processed according to a validated LC-MS/MS multi-residue method for the determination of β-lactams compounds in animal tissue [24,25], modifying the elution stage of the SPE. In order to determine if the method for β-lactams was also valid for quinolones, recoveries from spiked muscle samples with the four studied quinolones were carried out. Results showed a recovery of 81.6% for ENR, 62.6% for CIP, 73.2% for DIF and 70.5% for SAR, which were considered acceptable values. Briefly, antibiotics were extracted from 4g (± 0.1mg) of minced chicken muscle with a mixture of 2mL of MilliQ water and 20mL of MeCN. After shaking for 2 min, the mixture was centrifuged at 3500 rpm (5 min) and the obtained hydroorganic extract was evaporated under N_2 stream in a TurboVap system at 35ºC until 2mL as final volume. 25mL of 0.050 mol L^{-1} phosphate solution at pH 5.0 was added to the remaining aqueous extract and the resulting mixture was processed by SPE. The Isolute ENV+ cartridges were activated with 2mL of MeOH, 2mL of MilliQ water and 2mL of 0.050 mol L^{-1} phosphate solution at pH 5.0. The muscle extract was then loaded to the

198 cartridge and washed with 3mL of phosphate solution at pH 5.0 and 1mL of MilliQ
199 water, followed by the elution of the analytes with 5mL of the hydroorganic solution
200 TFA:H_2O:MeCN (2:23:75, v/v/v) and 1mL of MeCN. The produced SPE eluates were
201 evaporated to dryness at 35ºC under N_2 stream and reconstituted with 200µL of MilliQ
202 water. Prior to injection, samples were filtered and stored at -20ºC.
203 An aliquot of 20µL and 10µL of the extracts were injected into the chromatographic
204 system for the LC-QqToF and LC-LTQ-Orbitrap experiments, respectively.

205

206 *2.4.4. Instrumental conditions*

207 LC-UV and LC-QqToF analyses were performed at a constant flow rate of 1.0 mL min^{-1}.
208 LC-LTQ-Orbitrap analyses were performed at a constant flow rate of 0.3 mL min^{-1}. In
209 all cases, the same binary solvent system was used: solvent A, 0.005 mol L^{-1} NH_4AcO
210 adjusted at pH 2.5 with HFo and solvent B, MeCN.
211 LC-UV analyses gradient system was programmed as follows: initially 12% B, from 0
212 to 7.5 min B was maintained at 12%, from 7.5 to 23.5 min B was linearly increased to
213 29% and from 23.5 to 25 min decreased to 28%. Finally B decreased to initial
214 conditions in 1 min and maintained at this percentage for 2 min. The detection was
215 carried out at 280 nm for all quinolones. Acquisition and data processing were
216 performed by ChemStation software Agilent Technologies (Waldbronn, Germany).
217 LC-QqToF analyses gradient system was programmed as follows: initially 14% B, from
218 0 to 5 min B increased to 21%, from 5 to 6 min B increased to 24%, from 6 to 7.5 min B
219 increased to 25%, from 7.5 to 9 min B increased to 54% and then maintained at 54% for
220 0.5 min. Finally B decreased to 14% in 0.5 min and maintained at this percentage for 3
221 min. A T-piece splitter (3:1) was used to reduce the flow-rate entering into the
222 electrospray ionization source. Working in positive ionization mode, optimized

instrument parameters settings were the following: Ion Spray (IS) voltage was 4500V; gas temperature 400 ºC; Declustering Potencial (DP) 60 V; Focusing Potencial (FP) 350 V and Declustering Potential 2 (DP2) 10 V. Mass spectrometry analyses were carried out on full-scan MS mode, working at a resolving power of 10000 and with a mass range of 100–1000 Da at a scan rate of 1s per spectrum. Analyst QS version 2.0 and Peak View 1.2 from Applied Biosystems (Toronto, Canada) were used for the acquisition and data processing, respectively.

LC-LTQ-Orbitrap analyses gradient system was programmed as follows: initial 3% B, from 0 to 5 min B increased to 25%, from 5 to 6 min B increased to 35%, from 6 to 7 min B increased to 55% and then maintained at this percentage for 1 min. Finally B decreased to 3% in 1.5 min and maintained at this percentage for 3 min. Mass spectrometry analyses were carried out on full-scan MS and product ion scan MS/MS modes with a mass range of 100–1000 Da. The resolving power was 30000 and 15000 for the full-scan and MS/MS events, respectively. Employing positive ionization mode, a multiple component detection method was used as a default values of the parameters settings to carry out the different experiments. A source voltage of 3500V and a capillary temperature of 300ºC were used as main parameters settings. Collision energy (HCD) of 40-70% was used for the MS/MS experiments. Acquisition and data processing were performed by Xcalibur 2.1 QualBrowser from Thermo Fisher Scientific (Hemel Hempstead, UK).

2.4.5. Data processing

Metabolites and TPs identification in the medicated chicken muscle samples were performed by processing the accurate-mass full-scan raw data by MMDF [26-28] using Peak View 1.2 from Applied Biosystems (Toronto, Canada). ENR (*m/z* 360.1718), CIP

(*m/z* 332.1405), the core substructure with *m/z* 263.0826, formed by the piperazine ring loss, and the glucuronide conjugation of ENR (*m/z* 536.2039), were used as MDF templates. The MDF window was set to ±40 mDa around the mass defects of the templates over a mass range of ±50 Da around the filter template masses. The use of MMDF technique as a pre-filter enabled the reduction of most of the false-positive peaks (endogenous components) and background interferences.

Once the data was filtered, comparison of mass spectral data between samples and blanks enabled to differentiate the metabolite ions of interest from interference ions in the biological matrix, especially those ions that show a very low intensity by LC-MS. The identification of the different TPs in the preliminary stability study was performed directly by comparison of mass spectral data from samples and blanks.

The confirmation and structure elucidation of the identified metabolites and TPs were carried out by the MS/MS spectrum generated by the product ion scan of each ion.

3. Results and discussion

3.1. Effect of pH and F/T cycles

Figure 1 shows the effect of pH on ENR, CIP, DIF and SAR after applying three F/T cycles for each pH value. Areas were obtained by LC-UV and rescaled to values between 0 and 1 (relative values) for each pH value and F/T cycle, which enabled a better visualization and interpretation of the variation of the compound depending on the pH or the number of applied F/T cycles. Rescaling was accomplished by dividing the area obtained for each pH value and F/T cycle by the larger area of those areas obtained for the compound. This procedure was carried out for each compound.

Considering that a degradation lower than 10% negligible, at extreme pH values, the compounds do not show significant degradation after applying three F/T cycles.

However, at pH values between 2.5-3.5 and 6.5, a degradation around 15-25% is observed for the four studied quinolones. At these pH values, significant degradation is observed after applying the first F/T cycle, whereas for the rest of the pH values, degradation is less pronounced when increasing the number of applied F/T cycles.

3.1.1. Transformations products

Table 1 shows a summary of the observed TPs from ENR, CIP, DIF and SAR standard solutions when were subjected to different conditions of pH and after applying three F/T cycles. In Table 1, mass spectral data and MS/MS spectrum for each compound are shown. Proposed structures for each compound are shown in Figures 2 and 3.

According to the structure for each compound, main degradation processes of ENR, CIP, DIF and SAR are piperazine ring and aromatic core transformations. Main degradation steps involved in the piperazine ring substituent were ring cleavage and once the ring has been cleaved, the resulted primary or secondary amine undergoes further degradation that leads to methylated, formylated and acetylated products in positions 1 and 4 of the piperazine ring. Other degradation conversions are oxidative steps (oxo-formation), hydroxylation and methylation in positions 2 and 3 of the piperazine ring, as well as N-oxidation, N-hydroxylation, N-formylation, N-acetylation, N-demethylation and N-deethylation, with or without subsequent ring cleavage, in position 4 of the piperazine ring. Aromatic core reactions were mainly based on the hydroxylation at the two available positions on the aromatic ring, as well as the defluorination of the molecule. Decarboxylated compound were also observed for ENR and SAR, as well as combinations of piperazine ring and aromatic core based reactions.

TPENR-1, TPENR-3, TPENR-5, TPENR-9, TPENR-10, TPENR-13, TPENR-14, TPENR-17, TPENR-18, TPCIP-1, TPCIP-4, TPDIF1, TPDIF-3, TPDIF-7, TPSAR-3 and

298 TPSAR-6 are quinolone structures described in literature as photo-degradation products in
299 environmental samples [6-12] and microbiological transformation products [13-20] but, to
300 our knowledge, the rest of the observed compounds have not been described previously.
301 From the intensity showed by LC-MS, the different compounds can be divided in three
302 groups. In the first group TPENR-20, TPCIP-5, TPDIF-13, TPSAR-11 and TPENR-21,
303 TPCIP-6, TPDIF-14, TPSAR-12 are included. Those ones are structure related compounds
304 and show the most intense signal. These compounds could be formed by quinolone
305 degradation and interaction with reagents present in the medium. The second group would
306 be formed by TPENR-3 (CIP) and TPDIF-3 (SAR), formed via N-desethylation and N-
307 desmethylacion of ENR and DIF, respectively, and TPENR-5, TPCIP-1, TPDIF-1 and
308 TPSAR-3, formed by piperazine ring cleavage (deethylation). In the third group would be
309 the rest of the compounds, which show a very low intensity.
310 Figure 4 shows the effect of pH on the main observed TPs for each quinolone. Peak
311 areas were rescaled following the same procedure indicated in section 3.1. As Figure 4
312 shows, all TPs were formed at all pH values and most of them show the same behavior
313 than ENR, CIP, DIF and SAR. At pH values between 2.5-3.5 and 6.5 were less formed
314 than for the rest of pH values, except for TPENR-20, TPCIP-5, TPDIF-13, TPSAR-11 and
315 TPENR-21, TPCIP-6, TPDIF-14, TPSAR-12, which show just the opposite behavior.
316 Therefore, the formation of those TPs could explain the behavior showed by the four
317 studied quinolones and the rest of TPs.
318
319 *3.2. Medicated animal samples*
320 Chicken muscle samples from medicated animals with ENR (explained in section 2.4.2)
321 were analyzed with the purpose of identifying those unknown metabolites and TPs
322 which could be present in the animal tissue and therefore, can lead to health risks when

pass to humans through the food chain. These metabolites and TPs could be formed by interaction with biological substances, biotransformation reactions that occur in the own animal (metabolism) or even originated by the complex sample treatment.

Table 2 shows a summary of the identified metabolites obtained from the chicken muscle samples from the medicated animals with ENR. In Table 2, mass spectral data, MS/MS spectrum and the proposed structure for each metabolite are shown.

According to the proposed structure for each metabolite shown in Table 2, main biotransformation processes of ENR due to the animal metabolism are piperazine ring transformations as occur in preliminary study. Piperazine ring cleavage (M1 and M3), piperazine ring cleavage and the subsequent addition of methyl and acetyl groups in positions 1 and 4 (M6 and M11), oxidation in position 2 (M8 and M14) and N-deethylation, N-demethylation, N-acetylation and N-hydroxylation in position 4 of the piperazine ring (M2, M5, M9 and M12) were observed. Aromatic core biotransformation reactions were also observed, mainly based on the hydroxylation of the aromatic ring and the defluorination of the molecule, with or without subsequent hydroxylation, such as M4, M10 and M13. Other biotransformation processes combined piperazine ring and aromatic core based reactions, such as M7 and M10.

The two most abundant observed metabolites were M2, formed by the N-desethylation of ENR, leading to ciprofloxacin [14,15,18,20,21], and M3, originated by the piperazine ring cleavage (deethylation), leading to desethylene-enrofloxacin [14,15,18,20,21]. Other metabolites which had a great abundance in the samples were M1, M4 and M10.

As for the grade of the animal metabolism, after four days of pharmacological treatment ends, the animal metabolized and excreted most of the metabolites. However, the supplied antibiotic (ENR) and some of the metabolites observed after three days of

pharmacological treatment (M1, M2, M3, M4 and M10) still remain in the animal muscle tissue.

As occur for ciprofloxacin (M2) and desethylene-enrofloxacin (M3), M1, M8, M9, M10 and M14 are quinolone structures described in literature as microbiological biotransformation products [14,15,18,20] and metabolite residues of ENR in animal tissues for human consumption [21], but M4, M5, M6, M7, M11, M12 and M13 have not been described previously in the literature

Metabolites M1, M2, M3, M6, M8, M9, M11, M12, M13 and M14 were also observed as TPs in the preliminary study (TPENR-1, TPENR-3, TPENR-5, TPENR-8, TPENR-9, TPENR-10, TPENR-13, TPENR-15, TPENR-16 and TPENR-17, respectively).

3.2.1. Structural elucidation of the main metabolites

In general, the loss of water $[M+H-H_2O]^+$, the loss of the carboxyl moiety $[M+H-CO_2]^+$ and the loss of the fluoride $[M+H-HF]^+$ are characteristic fragmentation pathways for fluoroquinolones [11,29]. Moreover, ENR in particular shows the loss of the cyclopropyl group $[M+H-C_3H_5^{\cdot}]^+$ and the N-desethylation followed by the degradation steps of the piperazinyl moiety $[M+H-C_2H_4\text{-}C_2H_5N]^+$ (see ENR in Table 2). Thus, the appearance of these fragmentations in the MS/MS spectrum can give hints, for example, at the existence of an intact carboxyl moiety or an intact piperazinyl moiety. Figure 5 shows the MS/MS spectra of the main metabolites.

The compound with *m/z* 263.0822 (Figure 5A) displayed all typical product ions of ENR, giving the loss of H_2O (*m/z* 245.0722), the loss of the cyclopropyl group (*m/z* 222.0436), decarboxylation and desaturation (*m/z* 217.0772), the combined loss of H_2O and the cyclopropyl group (*m/z* 204.0330) and the combined loss of the carboxyl group, a carbonyl group and the partial cyclopropyl group cleavage (*m/z* 177.0824), except for

372 the degradation of the piperazinyl moiety. Consequently, it reflects an ENR derivative
373 with a NH_3 substituent in position 7 as is the case for M1 (Table 2).
374 MS/MS measurements of the compound with *m/z* 332.1405 (Figure 5B) showed typical
375 fragmentation pathways such as the loss of H_2O leading to *m/z* 314.1302, the loss of the
376 carboxyl group resulting in *m/z* 288.1509 and the combined loss of the carboxyl group
377 and fluoride yielding *m/z* 268.1445. These fragments do not hint any plausible structure,
378 but the combined fragments of *m/z* 245.1087, originated by the loss of the carboxyl
379 group and the piperazinyl moiety, *m/z* 231.0928 equivalent to the loss of the carboxyl
380 group and the further degradation of the piperazine ring and *m/z* 204.0693, which
381 combines the loss of the carboxyl group, the piperazinyl moiety and the loss of the
382 cyclopropyl group, reflects the absence of a N-ethyl group in position 4 of the molecule,
383 which indicates that the compound with *m/z* 332.1405 can be assigned to the proposed
384 structure for M2 (Table 2).
385 The compound with *m/z* 334.1556 showed also typical fragmentation pathways (Figure
386 5C) such as the loss of fluoride leading to *m/z* 314.1500, the combined loss of H_2O and
387 fluoride yielding *m/z* 296.1395, the combined loss of the carboxyl group, desaturation
388 and fluoride resulting in *m/z* 268.1445 and the combined loss of H_2O, fluoride and the
389 cyclopropyl group giving the fragment with *m/z* 255.1003. The fragments with *m/z*
390 289.0983, originated by the loss of an ethyl group and NH_3 and *m/z* 245.1087 due to the
391 combined loss of the carboxyl group, an ethyl group and NH_3, and moreover, the
392 fragments with *m/z* 263.0827 and *m/z* 219.0928 in whose structures remains only a
393 primary amine as substituent in position 7, in combination with the lack of the typical
394 piperazinyl moiety fragment ions, suggests the piperazine ring cleavage, which is in
395 agreement with the proposed structure for M3 (Table 2).

The substance with *m/z* 342.1806 (Figure 5D) possessed the fragment ions of the loss of H_2O, which leads to *m/z* 324.1707, the loss of the carboxyl group giving *m/z* 298.1912 and the combined loss of H_2O, followed by N-desethylation and desethylation due to the piperazine ring cleavage resulting in *m/z* 268.1081, as well as the combined loss of the carboxyl group, N-desethylation and degradation of the piperazinyl moiety yielding *m/z* 227.1178, and the decarboxylation, N-desethylation and further degradation of the piperazinyl moiety leading to *m/z* 213.1021. However, the lack of the typical fluoride loss fragment ion suggests the absence of the fluoride according to the proposed structure for M4 (Table 2).

MS/MS measurements of the compound with *m/z* 374.1701 (Figure 5E) show the loss of H_2O (*m/z* 356.1602), the loss of the carboxyl group (*m/z* 330.1970), the combined degradation of the piperazinyl moiety and N-desethylation (*m/z* 303.0971) and the combined N-desethylation, loss of H_2O and the degradation of the piperazinyl moiety (*m/z* 285.0868). Furthermore, N-desethylation and a further degradation of the piperazine ring give the fragment with *m/z* 277.0817 and the combined loss of the carboxyl group, desaturation, N-desethylation and the piperazinyl moiety leads to *m/z* 257.0919. Subtraction between molecular formulas of ENR and the identified *m/z* 374.1701, obtained by the QualBrowser software from Thermo Fisher Scientific, gives a difference of $[M+2H+2O-F]^+$, which suggests the defluorination of the molecule and the addition of two hydroxyl groups. The lack of the typical fluoride loss fragment ion and the absence of the loss of a hydroxyl group from the combined piperazine ring fragments ions in the MS/MS spectrum, suggest that the metabolite was originated by the replacement of the fluoride for a hydroxyl group and the hydroxylation of the aromatic core in one of the two available positions, as reflects the proposed structure for M10 shown in Table 2.

4. Conclusions

A total of 21 TPs from ENR, 6 TPs from CIP, 14 TPs from DIF and 12 TPs from SAR were identified due to the pH shock and F/T cycles, where the formation of CIP and SAR, from ENR and DIF, respectively, the formation of desethylene-quinolone and the formation of TPENR-20, TPCIP-5, TPDIF-13, TPSAR-11 and TPENR-21, TPCIP-6, TPDIF-14, TPSAR-12, were the most remarkable observed compounds. The four quinolones showed a sharp instability at pH values between 2.5-3.5 and 6.5, which could be explained by the formation of two related structure compounds for each one (TPENR-20, TPCIP-5, TPDIF-13, TPSAR-11 and TPENR-21, TPCIP-6, TPDIF-14, TPSAR-12).

In the analysis of the chicken muscle samples from the medicated animals with ENR, a total of 14 metabolites were identified. Formation of CIP (M2) and desethylene-enrofloxacin (M3) were the most abundant observed metabolites. The animal metabolized and excreted most of the metabolites after four days the medical treatment ended, but residues of ENR and some metabolites (M1, M2, M3, M4 and M10) still remained in the animal muscle tissue.

Regarding to the main degradation and biotransformation processes of quinolones observed in both studies, stand out piperazine ring and aromatic core based reactions.

Acknowledgements

The authors are gratefully acknowledged for the financial support of the Spanish Ministry of Spanish Government (Project CTQ2010-19044/BQU). We also wish to acknowledge M. Rey and A. Villa, from PONDEX S.A. poultry farm, Juneda (Lleida), for kind donation of medicated chicken samples.

F. J. Morales-Gutiérrez would like to thank the APIF fellowship from the University of Barcelona.

References

[1] C. Blasco, C. M. Torres, Y. Picó. Progress in analysis of residual antibacterials in food. Trends Anal. Chem. 26 (2007) 895-913.

[2] A.A.M. Stolker, U.A.Th. Brunkman. Analytical strategies for residue analysis of veterinary drugs and growth-promoting agents in food-producing animals-a review. J. Chromatogr. A. 1067 (2005) 15-53.

[3] A. Fàbrega, J. Sánchez-Céspedes, S. Soto, J. Vila. Quinolone resistance in the food chain. Int. J. Antimicrob. Agents. 31 (2008) 307-315.

[4] EU (2010) Commission Regulation (EU) 37/2010 amending Annexes I to IV to Council Regulation (EEC) No 2377/90 on pharmacologically active substances and their classification regarding maximum residue limits in foodstuffs of animal origin. Off. J. Eur. Commun. 2010 L15:1 (http://europa.eu.int).

[5] R. Companyó, M. Granados, J. Guiteras, M.D. Prat. Antibiotics in food: Legislation and validation of analytical methodologies. Anal. Bioanal. Chem. 395 (2009) 877-891.

[6] M. Sturini, A. Speltini, F. Maraschi, A. Profumo, L. Pretali, E. Fasani, A. Albini. Sunlight-induced degradation of soil-adsorbed veterinary antimicrobials Marbofloxacin and Enrofloxacin. Chemosphere. 86 (2012) 130-137.

[7] Y. Li, J. Niu, W. Wang. Photolysis of Enrofloxacin in aqueous systems under simulated sunlight irradiation: Kinetics, mechanism and toxicity of photolysis products. Chemosphere. 85 (2011) 892-897.

[8] T. Paul, M.C. Dodd, T.J. Strathmann. Photolytic and photocatalytic decomposition of aqueous ciprofloxacin: Transformation products and residual antibacterial activity. Water Res. 44 (2010) 3121-3132.

[9] M. Sturini, A. Speltini, F. Maraschi, A. Profumo, L. Pretali, E. Fasani, A. Albini. Photochemical Degradation of Marbofloxacin and Enrofloxacin in Natural Waters. Environ. Sci. Technol. 44 (2010) 4564-4569.

[10] S. Kusari, D. Prabhakaran, M. Lamshoft, M. Spiteller. In vitro residual anti-bacterial activity of difloxacin, sarafloxacin and their photoproducts after photolysis in water. Environ. Pollut. 157 (2009) 2722-2730.

[11] P. Calza, C. Medana, F. Carbone, V. Giancotti, C. Characterization of intermediate compounds formed upon photo-induced degradation of quinolones by high-performance liquid chromatography/high-resolution multiple-stage mass spectrometry. Rapid Commun. Mass Spectrom. 22 (2008) 1533-1552.

[12] E. Turiel, G. Bordin, A. Rodriguez. Study of the evolution and degradation products of ciprofloxacin and oxolinic acid in river water samples by HPLC-UV/MS/MS-MS. J. Environ. Monit. 7 (2005) 189-195.

[13] A. Prieto, M. Moeder, R. Rodil, L. Adrian, E. Marco-Urrea. Degradation of the antibiotics norfloxacin and ciprofloxacin by a white-rot fungus and identification of degradation products. Bioresour. Technol. 102 (2011) 10987-10995.

[14] W. Karl, J. Schneider, H.G. Wetzstein. Outlines of an "exploding" network of metabolites generated from the fluoroquinolone enrofloxacin by the brown rot fungus Gloeophyllum striatum. Appl. Microbiol. Biotechnol. 71 (2006) 101-113.

[15] H.G. Wetzstein, J. Schneider, W. Karl. Patterns of metabolites produced from the fluoroquinolone enrofloxacin by Basidiomycetes indigenous to agricultural sites. Appl. Microbiol. Biotechnol. 71 (2006) 90-100.

[16] I.A. Parshikov, T.M. Heinze, J.D. Moody, J.P. Freeman, A.J. Williams, J.B. Sutherland The fungus Pestalotiopsis guepini as a model for biotransformation of ciprofloxacin and norfloxacin. Appl. Microbiol. Biotechnol. 56 (2001) 474-477.

[17] I.A. Parshikov, J.P. Freeman, J.O. Lay, J.D. Moody, A.J. Williams, R.D. Beger, J.B. Sutherland. Metabolism of the veterinary fluoroquinolone sarafloxacin by the fungus Mucor ramannianus. J. Ind. Microbiol. Biotechnol. 26 (2001) 140-144.

[18] I.A. Parshikov, J.P. Freeman, J.O. Lay, R.D. Beger, A.J. Williams, J.B. Sutherland Microbiological transformation of enrofloxacin by the fungus Mucor ramannianus. Appl. Environ. Microbiol. 66 (2000) 2664-2667.

[19] H. Wetzstein, M. Stadler, H. Tichy, A. Dalhoff, W. Karl. Degradation of ciprofloxacin by Basidiomycetes and identification of metabolites generated by the brown rot fungus Gloeophyllum striatum. Appl. Environ. Microbiol. 65 (1999) 1556-1563.

[20] H. Wetzstein, N. Schmeer, W. Karl. Degradation of the fluoroquinolone enrofloxacin by the brown rot fungus Gloeophyllum striatum: identification of metabolites. Appl. Environ. Microbiol. 63 (1997) 4272-4281.

[21] S.B. Turnipseed, J.M. Storey, S.B. Clark, K.E Miller. Analysis of Veterinary Drugs and Metabolites in Milk Using Quadrupole Time-of-Flight Liquid Chromatography-Mass Spectrometry. J. Agric. Food Chem. 59 (2011) 7569-7581.

[22] P. Sukul, M. Lamshoeft, S. Kusari, S. Zuehlke, M. Spiteller. Metabolism and excretion kinetics of ^{14}C-labeled and non-labeled difloxacin in pigs after oral administration, and antimicrobial activity of manure containing difloxacin and its metabolites. Environ. Res. 109 (2009) 225-231.

[23] A. Anadon, M.R. Martinez-Larranaga, J. Iturbe, M.A. Martinez, M.J. Diaz, M.T. Frejo, M. Martinez. Pharmacokinetics and residues of ciprofloxacin and its metabolites in broiler chickens. Res. Vet. Sci. 712 (2001) 101-109.

[24] C.A. Macarov, L. Tong, M. Martinez-Huelamo, M. P. Hermo, E. Chirila, Y.X. Wang, D. Barron, J Barbosa. Multi residue determination of the penicillins regulated by

520 the European Union, in bovine, porcine and chicken muscle, by LC-MS/MS. Food
521 Chem. 135 (2012) 2612-2621.
522 [25] R. Perez-Burgos, E.M. Grzelak, G. Gokce, J. Saurina, J. Barbosa, D. Barron.
523 Quechers methodologies as an alternative to solid phase extraction (SPE) for the
524 determination and characterization of residues of cephalosporins in beef muscle using
525 LC-MS/MS. J. Chromatogr. B 899 (2012) 57-65.
526 [26] H. Zhang, D. Zhang, K. Ray, M. Zhu. Mass defect filter technique and its
527 applications to drug metabolite identification by high-resolution mass spectrometry. J.
528 Mass Spectrom. 44 (2009) 999-1016.
529 [27] M. Zhu, L. Ma, D. Zhang, K. Ray, W. Zhao, W.G. Humphreys, G. Skiles, M.
530 Sanders, H. Zhang. Detection and characterization of metabolites in biological matrices
531 using mass defect filtering of liquid chromatography/high resolution mass spectrometry
532 data. Drug Metab. Dispos. 34 (2006) 1722-1733.
533 [28] H. Zhang, D. Zhang, K. Ray. A software filter to remove interference ions from
534 drug metabolites in accurate mass liquid chromatography/mass spectrometric analyses.
535 J. Mass Spectrom. 38 (2003) 1110-1112.
536 [29] D.A. Volmer, B. Mansoori, S.J. Locke. Study of 4-quinolone antibiotics in
537 biological samples by short-column liquid chromatography coupled with electrospray
538 ionization tandem mass spectrometry. Anal. Chem. 69 (1997) 4143-4155.

Figure captions

Figure 1. Effect of pH and F/T cycles on standard solutions of ENR, CIP, DIF and SAR.

Symbols:

Figure 2. Proposed structures for the identified TPs from ENR (A) and CIP (B) standard solutions at different pH values.

Figure 3. Proposed structures for the identified TPs from DIF (A) and SAR (B) standard solutions at different pH values.

Figure 4. Effect of pH on major TPs.

Figure 5. MS/MS spectra of the main identified metabolites of ENR in the medicated chicken samples. A) M1, B) M2, C) M3, D) M4 and E) M10.

Table 1. Mass spectral data and MS/MS spectrum of the identified TPs from ENR, CIP, DIF and SAR due to pH shock and F/T cycles.

Compound	$[M+H]^+_{exp}$	RT (min)	Molecular Formula	$[M+H]^+_{theo}$	*m/z* error (ppm)	MS/MS spectrum
ENR	360.1715	4.90	$[C_{19}H_{23}N_3O_3F]^+$	360.17180	-0.8	360.1719, 342.1612, 340.1656, 316.1820, 286.0986, 257.1085, 245.1085, 231.0928
TPENR-1*	263.0820	6.79	$[C_{13}H_{12}N_2O_3F]^+$	263.08265	-2.5	263.0829, 245.0722, 222.0436, 217.0772, 204.0330, 177.0824
TPENR-2	316.1813	4.20	$[C_{18}H_{23}N_3OF]^+$	316.18197	-2.1	316.1829, 296.1767, 268.1451, 260.1202, 245.1092, 231.0934, 204.0698
TPENR-3*	332.1407	4.60	$[C_{17}H_{19}N_3O_3F]^+$	332.14050	0.6	332.1407, 314.1302, 288.1509, 268.1445, 245.1087, 231.0928, 204.0693
TPENR-4	334.1187	6.47	$[C_{16}H_{17}N_3O_4F]^+$	334.11976	-3.2	334.1195, 316.1090, 299.0842, 289.0970, 271.0874, 263.0826, 245.0720, 217.0406
TPENR-5*	334.1553	4.44	$[C_{17}H_{21}N_3O_3F]^+$	334.15615	-2.5	334.1561, 314.1500, 296.1395, 289.0983, 268.1445, 263.0827, 255.1003, 245.1087, 219.0928
TPENR-6	348.1346	6.10	$[C_{17}H_{19}N_3O_4F]^+$	348.13541	-2.3	348.1352, 330.1248, 302.1298, 289.0976, 287.1428, 285.1267, 245.1084
TPENR-7	348.1353	6.64	$[C_{17}H_{19}N_3O_4F]^+$	348.13541	-0.3	348.1352, 330.1246, 313.1003, 288.1152, 271.0876, 263.0822, 230.0483, 217.0406
TPENR-8*	348.1710	4.78	$[C_{18}H_{23}N_3O_3F]^+$	348.17180	-2.3	348.1718, 304.1818, 273.1269, 245.1084, 233.1084, 219.0927, 205.0771
TPENR-9*	374.1498	3.99	$[C_{19}H_{21}N_3O_4F]^+$	374.15106	-3.4	374.1510, 356.1411, 346.1557, 314.0937, 289.0981, 286.0985, 275.0827, 271.0877, 257.0724
TPENR-10*	374.1502	7.49	$[C_{19}H_{21}N_3O_4F]^+$	374.15106	-2.3	374.1511, 356.1406, 332.1029, 314.1301, 295.0951, 272.0829, 243.0562, 231.0564
TPENR-11	374.1865	5.24	$[C_{20}H_{25}N_3O_3F]^+$	374.18745	-2.5	374.1871, 356.1765, 330.1974, 302.1659, 286.0980, 271.1239, 259.1241, 245.1086, 205.0770
TPENR-12	376.1294	7.61	$[C_{18}H_{19}N_3O_5F]^+$	376.13033	-2.5	376.1306, 348.1353, 334.1187, 330.1247, 316.1086, 289.0982, 262.0748
TPENR-13*	376.1660	4.60	$[C_{19}H_{23}N_3O_4F]^+$	376.16671	-1.9	376.1668, 358.1561, 346.1548, 289.0983, 275.0824, 262.0749, 244.1012
TPENR-14	376.1657	5.00	$[C_{19}H_{23}N_3O_4F]^+$	376.16671	-2.7	376.1668, 358.1558, 332.1765, 305.0930, 301.1216, 261.1034, 233.0720
TPENR-15*	376.1662	5.27	$[C_{19}H_{23}N_3O_4F]^+$	376.16671	-1.4	376.1669, 359.1639, 344.1404, 330.1614, 315.1740, 300.1507, 287.1429
TPENR-16*	376.1655	5.77	$[C_{19}H_{23}N_3O_4F]^+$	376.16671	-3.2	376.1666, 332.1767, 301.1219, 261.1036, 247.0879, 220.0642
TPENR-17*	388.1297	6.64	$[C_{19}H_{19}N_3O_5F]^+$	388.13033	-1.6	388.1305, 360.1367, 348.0995, 342.1262, 330.0885, 320.1048, 302.0571
TPENR-18	390.1449	6.75	$[C_{19}H_{21}N_3O_5F]^+$	390.14598	-2.8	390.1472, 372.1361, 362.1514, 320.1053, 305.0936, 291.0783, 273.0674, 259.0519, 231.0568
TPENR-19	390.1449	7.08	$[C_{19}H_{21}N_3O_5F]^+$	390.14598	-2.8	390.1468, 372.1359, 362.1518, 320.1045, 299.0839, 291.0781, 273.0674, 259.0519, 231.0568
TPENR-20	462.1595	0.50	$[C_{20}H_{24}N_5O_8]^+$	462.16194	-5.3	462.1621, 444.1511, 436.1827, 418.1723
TPENR-21	490.1560	0.50	$[C_{21}H_{24}N_5O_9]^+$	490.15685	-1.7	490.1562, 476.1408, 448.1459, 422.1668, 404.1563, 394.1721, 378.1770, 376.1612, 360.1663
CIP	332.1405	4.70	$[C_{17}H_{19}N_3O_3F]^+$	332.14050	0.0	332.1407, 314.1302, 312.1345, 288.1509, 268.1445, 245.1087, 231.0928, 204.0693
TPCIP-1	306.1241	4.31	$[C_{15}H_{17}N_3O_3F]^+$	306.12485	-2.4	306.1255, 288.1148, 286.1190, 268.1084, 263.0830, 245.0722, 236.0595, 227.0692, 217.0410
TPCIP-2	346.1188	5.96	$[C_{17}H_{17}N_3O_4F]^+$	346.11976	-2.8	346.1196, 328.1087, 284.1186, 275.0824, 257.0721, 242.0721, 229.0771
TPCIP-3	346.1548	4.75	$[C_{18}H_{21}N_3O_3F]^+$	346.15615	-3.9	346.1559, 328.1457, 302.1663, 285.1269, 257.1085, 245.1084, 231.0928, 204.0691
TPCIP-4	360.1344	7.35	$[C_{18}H_{19}N_3O_4F]^+$	360.13541	-2.8	360.1351, 342.1221, 318.0888, 301.0848, 286.0984, 272.0826, 261.0663, 248.0589, 243.0562
TPCIP-5	434.1297	0.46	$[C_{18}H_{20}N_5O_8]^+$	434.13064	-2.2	434.1310, 416.1203, 408.1516, 390.1413
TPCIP-6	462.1257	0.46	$[C_{19}H_{20}N_5O_9]^+$	462.12555	0.3	462.1259, 448.1092, 420.1149, 394.1356, 376.1251, 366.1404, 350.1456, 348.1300, 332.1349
DIF	400.1466	5.43	$[C_{21}H_{20}N_3O_3F_2]^+$	400.14672	-0.3	400.1469, 382.1362, 356.1572, 336.1508, 311.0991, 299.0993, 285.0835
TPDIF-1	374.1310	5.21	$[C_{19}H_{18}N_3O_3F_2]^+$	374.13107	-0.2	374.1317, 354.1253, 343.0894, 336.1148, 325.0787, 317.0738, 308.1198, 299.0994, 280.1248
TPDIF-2	382.1557	5.20	$[C_{21}H_{21}N_3O_3F]^+$	382.15615	-1.2	382.1566, 364.1460, 338.1665, 321.1276, 308.1559, 293.1086, 281.1088, 267.0930
TPDIF-3	386.1308	5.34	$[C_{20}H_{18}N_3O_3F_2]^+$	386.13107	-0.7	386.1316, 366.1254, 342.1416, 322.1352, 299.0993, 285.0836, 279.0930
TPDIF-4	414.1250	4.69	$[C_{21}H_{18}N_3O_4F_2]^+$	414.12599	-2.4	414.1262, 386.1316, 368.1200, 347.1063, 343.0894, 329.0734, 325.0784, 311.0627

TPDIF-5	414.1616	5.68	$[C_{22}H_{22}N_3O_3F_2]^+$	414.16237	-1.9	414.1622, 370.1726, 339.1176, 313.1146, 299.0989, 285.0835
TPDIF-6	416.1401	4.78	$[C_{21}H_{20}N_3O_4F_2]^+$	416.14164	-3.7	416.1417, 398.1300, 371.0840, 343.0895, 327.0938, 299.0990
TPDIF-7	416.1413	5.05	$[C_{21}H_{20}N_3O_4F_2]^+$	416.14164	-0.8	416.1422, 398.1316, 386.1314, 353.1170, 343.0891, 329.0732, 316.0657
TPDIF-8	416.1403	5.45	$[C_{21}H_{20}N_3O_4F_2]^+$	416.14164	-3.2	416.1417, 398.1311, 372.1522, 350.0941, 315.0936, 301.0785
TPDIF-9	416.1410	5.82	$[C_{21}H_{20}N_3O_4F_2]^+$	416.14164	-1.5	416.1416, 372.1521, 359.0841, 341.0733, 315.0943, 287.0628, 274.0675
TPDIF-10	430.1203	5.72	$[C_{21}H_{18}N_3O_5F_2]^+$	430.12090	-1.4	430.1218, 402.1264, 373.0671, 356.0848, 343.0892, 329.0734, 317.0734, 299.0994
TPDIF-11	430.1208	7.15	$[C_{21}H_{18}N_3O_5F_2]^+$	430.12090	-0.2	430.1210, 412.1107, 402.1258, 384.1161, 356.0843, 345.0679, 327.0577, 317.0730, 299.0629
TPDIF-12	430.1210	7.36	$[C_{21}H_{18}N_3O_5F_2]^+$	430.12090	0.2	430.1209, 412.1100, 402.1260, 384.1164, 356.0844, 345.0680, 327.0572, 317.0732
TPDIF-13	502.1363	0.52	$[C_{22}H_{21}N_5O_8F]^+$	502.13687	-1.1	502.1365, 484.1268, 476.1569, 458.1472
TPDIF-14	530.1308	0.52	$[C_{23}H_{21}N_5O_9F]^+$	530.13178	-1.8	530.1312, 516.1155, 488.1219, 462.1418, 444.1317, 434.1475, 418.1526, 416.1359, 400.1422
SAR	386.1311	5.38	$[C_{20}H_{18}N_3O_3F_2]^+$	386.13107	0.1	386.1315, 368.1206, 366.1249, 342.1415, 340.1260, 322.1351, 299.0992, 285.0836
TPSAR-1	318.0566	7.92	$[C_{16}H_{10}NO_4F_2]^+$	318.05724	-2.0	318.0574, 300.0467, 272.0518, 256.0568, 244.0569, 224.0505
TPSAR-2	342.1412	4.91	$[C_{19}H_{18}N_3OF_2]^+$	342.14125	-0.1	342.1417, 322.1353, 299.0994, 294.1042, 285.0837
TPSAR-3	360.1154	5.15	$[C_{18}H_{16}N_3O_3F_2]^+$	360.11542	-0.1	360.1159, 343.0893, 340.1096, 322.0990, 317.0737, 299.0993, 294.1041, 279.0931, 266.1091
TPSAR-4	398.1498	5.31	$[C_{21}H_{21}N_3O_4F]^+$	398.15106	-3.2	398.1516, 380.1409, 354.1615, 337.1221, 311.1193, 297.1037, 281.0724
TPSAR-5	402.1247	5.11	$[C_{20}H_{18}N_3O_4F_2]^+$	402.12599	-3.2	402.1265, 382.1206, 364.1092, 352.1102, 343.0894, 329.0737, 316.0658
TPSAR-6	402.1249	7.50	$[C_{20}H_{18}N_3O_4F_2]^+$	402.12599	-2.7	402.1264, 384.1160, 343.0887, 317.0735, 299.0624, 271.0675
TPSAR-7	414.1616	5.95	$[C_{22}H_{22}N_3O_3F_2]^+$	414.16237	-1.9	414.1631, 386.1315, 366.1255, 343.0895, 325.0786, 299.0994
TPSAR-8	416.1042	6.59	$[C_{20}H_{16}N_3O_5F_2]^+$	416.10525	-2.5	416.1057, 388.1107, 372.1165, 342.0683, 329.0745, 316.0662, 299.0651
TPSAR-9	416.1053	6.84	$[C_{20}H_{16}N_3O_5F_2]^+$	416.10525	0.1	416.1058, 388.1111, 370.1005, 345.0686, 327.0576, 318.0578, 299.0632
TPSAR-10	428.1414	8.03	$[C_{22}H_{20}N_3O_4F_2]^+$	428.14164	-0.6	428.1415, 410.1316, 386.1309, 366.1376, 343.0888, 329.0730, 325.0781
TPSAR-11	488.1210	0.51	$[C_{21}H_{19}N_5O_8F]^+$	488.12122	-0.5	488.1219, 470.1106, 462.1424, 444.1313
TPSAR-12	516.1158	0.51	$[C_{22}H_{19}N_5O_9F]^+$	516.11613	-0.6	516.1165, 502.0996, 474.1052, 448.1265, 430.1160, 420.1310, 404.1363, 402.1210, 386.1261

(*) TPs from ENR also identified as metabolites in the chicken muscle samples (M1, M2, M3, M6, M8, M9, M11, M12, M13 and M14, respectively)

Table 2. Mass spectral data, proposed structures and MS/MS spectrum for the identified metabolites of ENR in the medicated chicken samples.

Compound	$[M+H]^+_{exp}$	RT (min)	Molecular Formula	$[M+H]^+_{theo}$	*m/z* error (ppm)	Proposed structure	MS/MS spectrum
ENR	360.1713	4.87	$[C_{19}H_{23}N_3O_3F]^+$	360.1718	-1.4	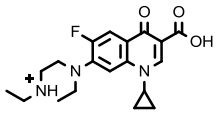	360.1721, 342.1613, 340.1656, 316.1818, 286.0985, 257.1084, 245.1084, 231.0927
M1	263.0822	6.77	$[C_{13}H_{12}N_2O_3F]^+$	263.08265	-1.7	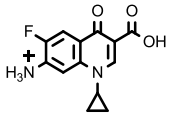	Figure 5A
M2	332.1405	4.59	$[C_{17}H_{19}N_3O_3F]^+$	332.14050	0.0	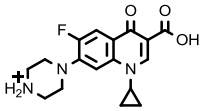	Figure 5B
M3	334.1556	4.41	$[C_{17}H_{21}N_3O_3F]^+$	334.15615	-1.6	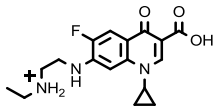	Figure 5C
M4	342.1806	4.29	$[C_{19}H_{24}N_3O_3]^+$	342.18122	-1.8	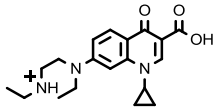	Figure 5D
M5	346.1552	4.65	$[C_{18}H_{21}N_3O_3F]^+$	346.15615	-2.7	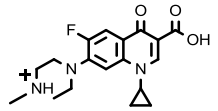	346.1563, 328.1462, 302.1665, 285.1278, 257.1086, 245.1087, 231.0929, 204.0693
M6	348.1716	4.77	$[C_{18}H_{23}N_3O_3F]^+$	348.17180	-0.6	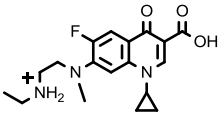	348.1718, 304.1818, 273.1269, 245.1084, 233.1084, 219.0927
M7	372.1915	4.75	$[C_{20}H_{26}N_3O_4]^+$	372.19178	-0.8	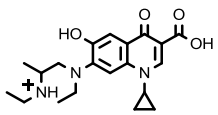	372.1919, 328.2017, 297.1470, 272.1400, 257.1284, 241.0971, 227.0813, 215.0811
M8	374.1500	3.70	$[C_{19}H_{21}N_3O_4F]^+$	374.15106	-2.8	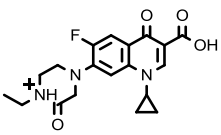	374.1510, 356.1411, 346.1557, 314.0937, 289.0981, 286.0985, 275.0827, 271.0877, 257.0724, 245.1093
M9	374.1496	7.47	$[C_{19}H_{21}N_3O_4F]^+$	374.15106	-3.9	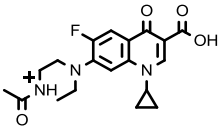	374.1511, 356.1406, 332.1029, 314.1301, 295.0951, 272.0829, 243.0562, 231.0564
M10	374.1701	4.69	$[C_{19}H_{24}N_3O_5]^+$	374.17105	-2.5	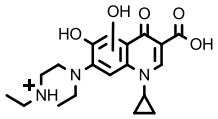	Figure 5E
M11	376.1673	4.58	$[C_{19}H_{23}N_3O_4F]^+$	376.16671	1.6	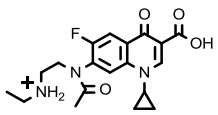	376.1668, 358.1561, 346.1548, 289.0983, 275.0824, 262.0749, 244.1012
M12	376.1664	5.23	$[C_{19}H_{23}N_3O_4F]^+$	376.16671	-0.8	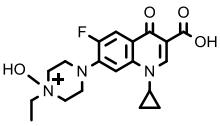	376.1669, 359.1639, 344.1404, 330.1614, 315.1740, 300.1507, 287.1429

M13	376.1657	5.84	$[C_{19}H_{23}N_3O_4F]^+$	376.16671	-2.7	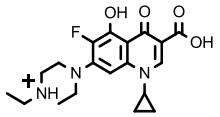	376.1666, 332.1767, 301.1219, 261.1036, 247.0879, 220.0642
M14	388.1302	6.63	$[C_{19}H_{19}N_3O_5F]^+$	388.13033	-0.3	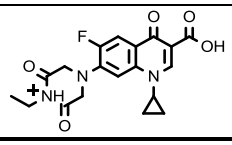	388.1305, 360.1367, 348.0995, 342.1262, 330.0885, 320.1048, 302.0571

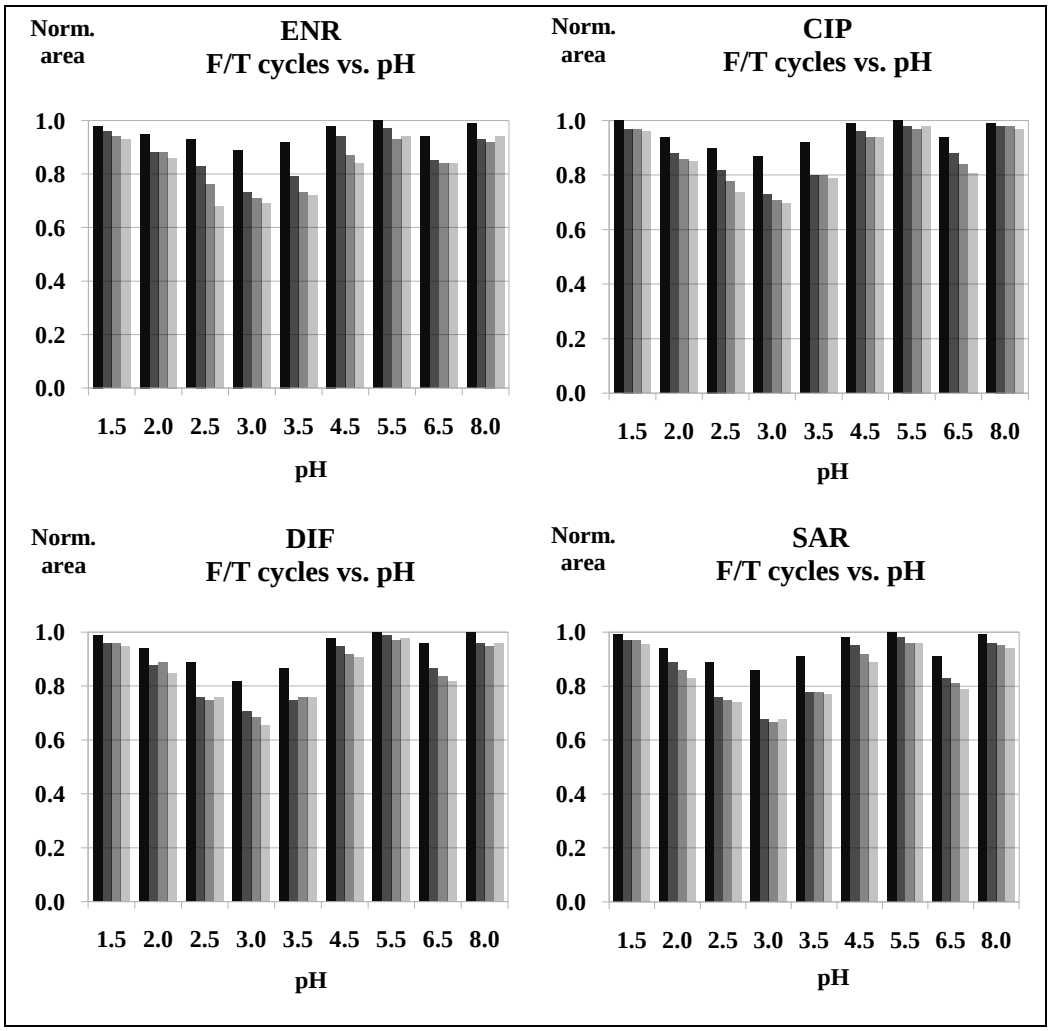
Norm. area
ENR
F/T cycles vs. pH
1.0
0.8
0.6
0.4
0.2
0.0
1.5 2.0 2.5 3.0 3.5 4.5 5.5 6.5 8.0
pH
Norm. area
CIP
F/T cycles vs. pH
1.0
0.8
0.6
0.4
0.2
0.0
1.5 2.0 2.5 3.0 3.5 4.5 5.5 6.5 8.0
pH
Norm. area
DIF
F/T cycles vs. pH
1.0
0.8
0.6
0.4
0.2
0.0
1.5 2.0 2.5 3.0 3.5 4.5 5.5 6.5 8.0
pH
Norm. area
SAR
F/T cycles vs. pH
1.0
0.8
0.6
0.4
0.2
0.0
1.5 2.0 2.5 3.0 3.5 4.5 5.5 6.5 8.0
pH

Figure 1.

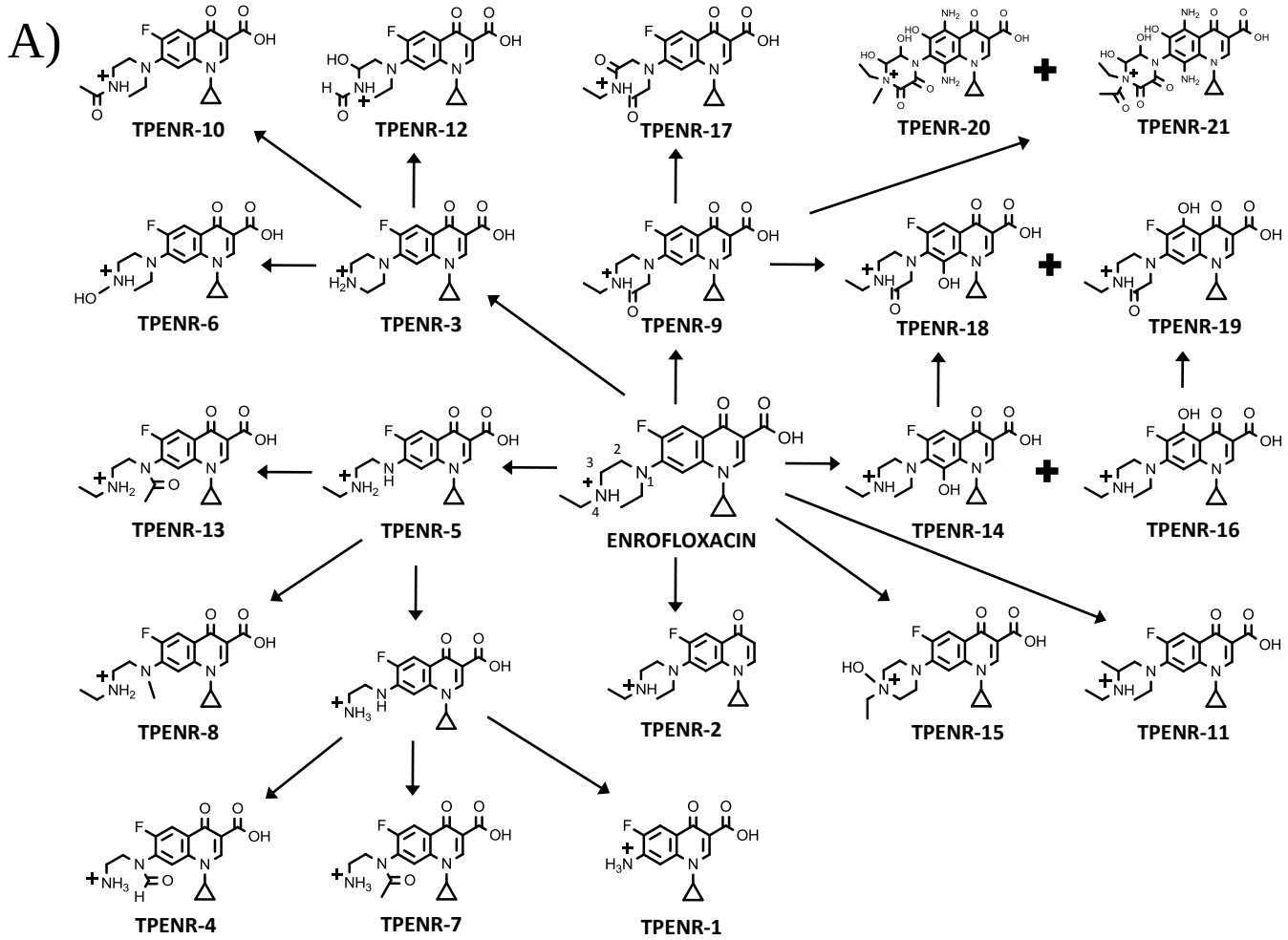
A)
TPENR-10
TPENR-12
TPENR-17
TPENR-20
TPENR-21
TPENR-6
TPENR-3
TPENR-9
TPENR-18
TPENR-19
TPENR-13
TPENR-5
ENROFLOXACIN
TPENR-14
TPENR-16
TPENR-8
TPENR-2
TPENR-15
TPENR-11
TPENR-4
TPENR-7
TPENR-1

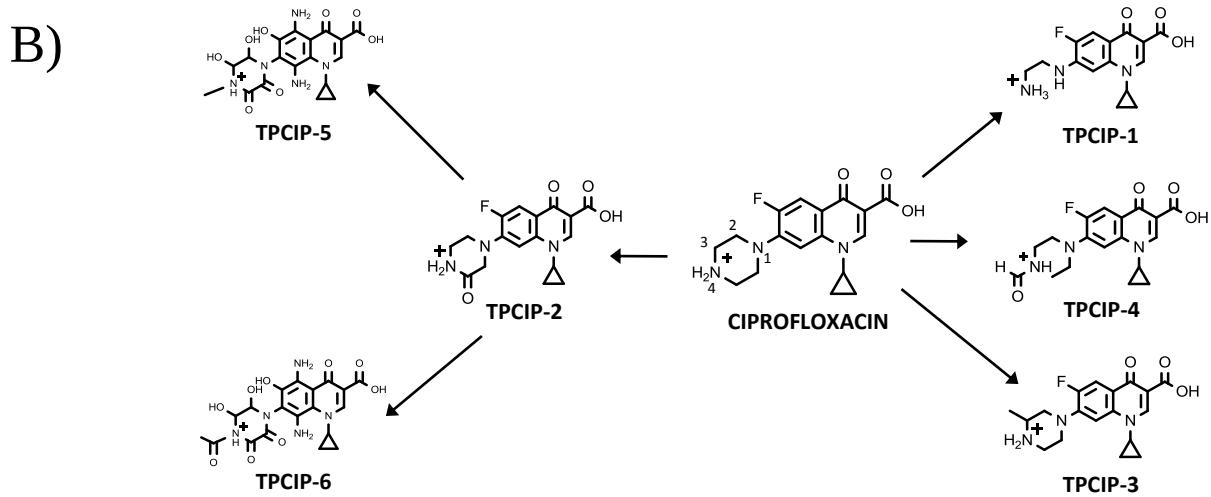
B)
TPCIP-5
TPCIP-1
TPCIP-2
CIPROFLOXACIN
TPCIP-4
TPCIP-6
TPCIP-3

Figure 2.

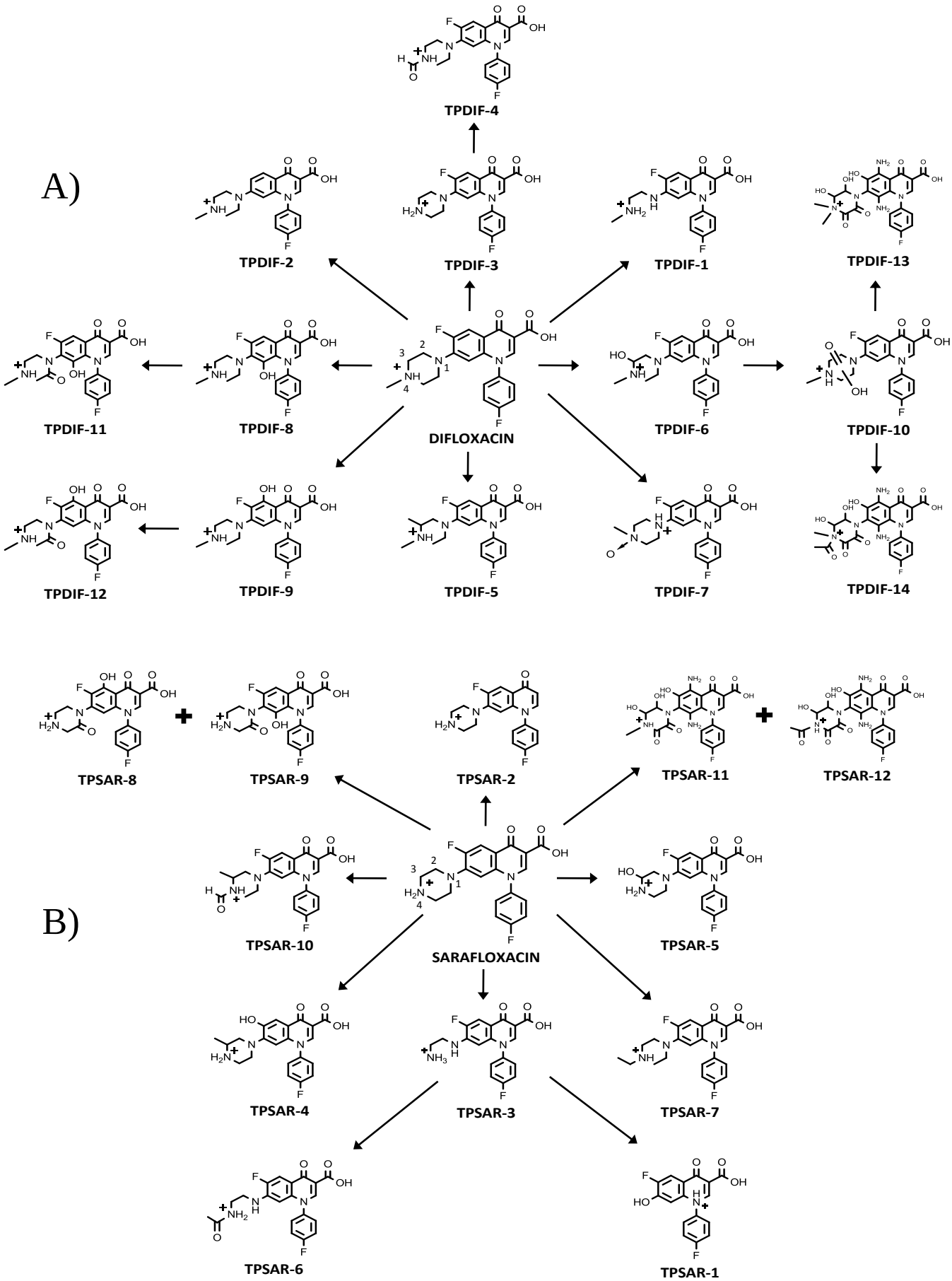
A)
TPDIF-4
TPDIF-2
TPDIF-3
TPDIF-1
TPDIF-13
TPDIF-11
TPDIF-8
DIFLOXACIN
TPDIF-6
TPDIF-10
TPDIF-12
TPDIF-9
TPDIF-5
TPDIF-7
TPDIF-14
B)
TPSAR-8
TPSAR-9
TPSAR-2
TPSAR-11
TPSAR-12
TPSAR-10
SARAFLOXACIN
TPSAR-5
TPSAR-4
TPSAR-3
TPSAR-7
TPSAR-6
TPSAR-1

Figure 3.

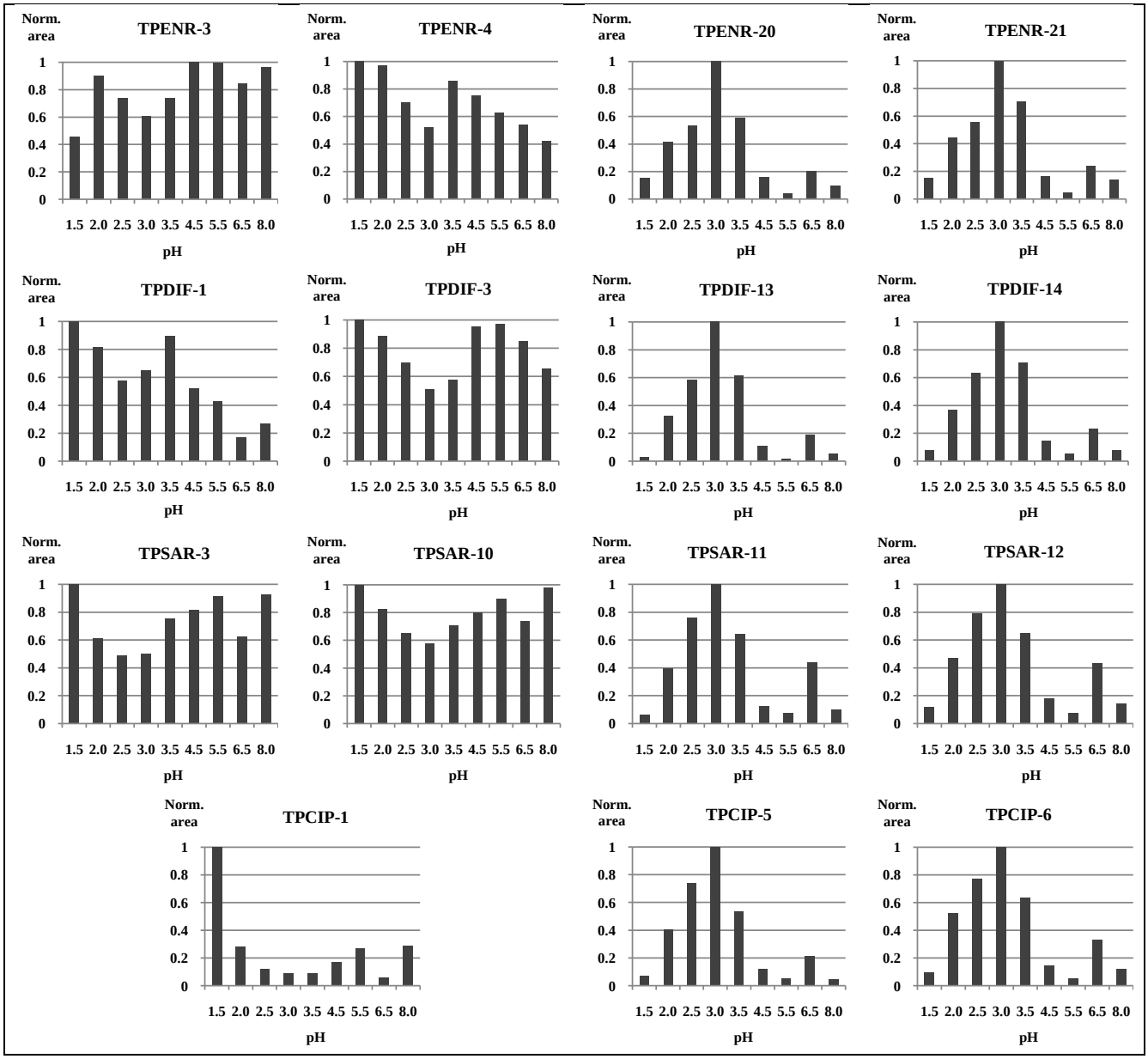
TPENR-3
TPENR-4
TPENR-20
TPENR-21
TPDIF-1
TPDIF-3
TPDIF-13
TPDIF-14
TPSAR-3
TPSAR-10
TPSAR-11
TPSAR-12
TPCIP-1
TPCIP-5
TPCIP-6
Norm. area
0
0.2
0.4
0.6
0.8
1
1.5 2.0 2.5 3.0 3.5 4.5 5.5 6.5 8.0
pH

Figure 4.

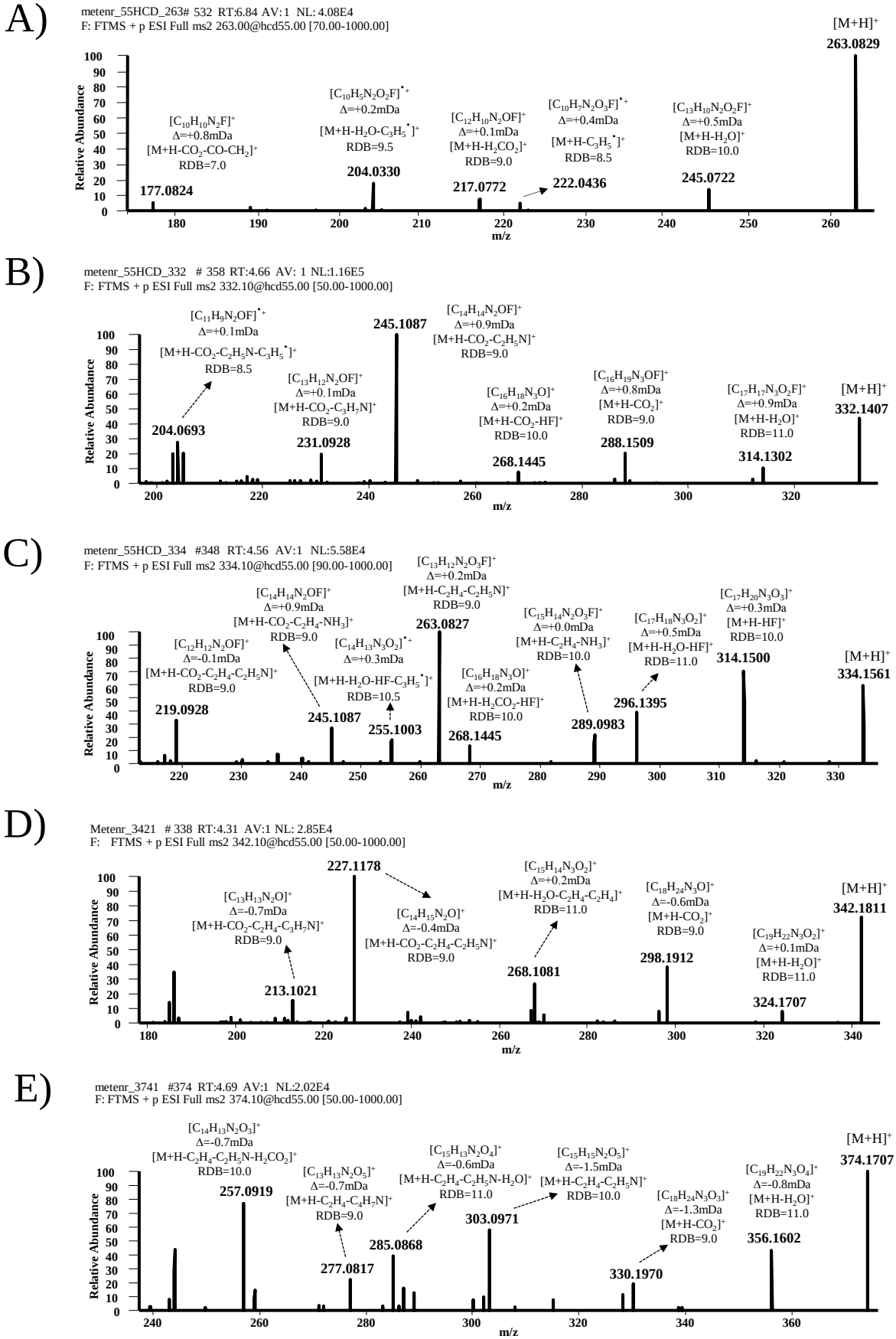
A)
metenr_55HCD_263# 532 RT:6.84 AV:1 NL: 4.08E4
F: FTMS + p ESI Full ms2 263.00@hcd55.00 [70.00-1000.00]
[M+H]+
263.0829
[C10H10N2F]+
Δ=+0.8mDa
[M+H-CO2-CO-CH2]+
RDB=7.0
177.0824
[C10H5N2O2F]•+
Δ=+0.2mDa
[M+H-H2O-C3H5•]+
RDB=9.5
204.0330
[C12H10N2OF]+
Δ=+0.1mDa
[M+H-H2CO2]+
RDB=9.0
217.0772
[C10H7N2O3F]•+
Δ=+0.4mDa
[M+H-C3H5•]+
RDB=8.5
222.0436
[C13H10N2O2F]+
Δ=+0.5mDa
[M+H-H2O]+
RDB=10.0
245.0722
Relative Abundance
m/z
B)
metenr_55HCD_332 # 358 RT:4.66 AV: 1 NL:1.16E5
F: FTMS + p ESI Full ms2 332.10@hcd55.00 [50.00-1000.00]
[C11H9N2OF]•+
Δ=+0.1mDa
[M+H-CO2-C2H5N-C3H5•]+
RDB=8.5
204.0693
245.1087
[C14H14N2OF]+
Δ=+0.9mDa
[M+H-CO2-C2H5N]+
RDB=9.0
[C13H12N2OF]+
Δ=+0.1mDa
[M+H-CO2-C3H7N]+
RDB=9.0
231.0928
[C16H18N3O]+
Δ=+0.2mDa
[M+H-CO2-HF]+
RDB=10.0
268.1445
[C16H19N3OF]+
Δ=+0.8mDa
[M+H-CO2]+
RDB=9.0
288.1509
[C17H17N3O2F]+
Δ=+0.9mDa
[M+H-H2O]+
RDB=11.0
314.1302
[M+H]+
332.1407
Relative Abundance
m/z
C)
metenr_55HCD_334 #348 RT:4.56 AV:1 NL:5.58E4
F: FTMS + p ESI Full ms2 334.10@hcd55.00 [90.00-1000.00]
[C13H12N2O3F]+
Δ=+0.2mDa
[M+H-C2H4-C2H5N]+
RDB=9.0
263.0827
[C14H14N2OF]+
Δ=+0.9mDa
[M+H-CO2-C2H4-NH3]+
RDB=9.0
[C12H12N2OF]+
Δ=-0.1mDa
[M+H-CO2-C2H4-C2H5N]+
RDB=9.0
219.0928
[C14H13N3O2]•+
Δ=+0.3mDa
[M+H-H2O-HF-C3H5•]+
RDB=10.5
245.1087
255.1003
[C15H14N2O3F]+
Δ=+0.0mDa
[M+H-C2H4-NH3]+
RDB=10.0
289.0983
[C16H18N3O]+
Δ=+0.2mDa
[M+H-H2CO2-HF]+
RDB=10.0
268.1445
[C17H18N3O2]+
Δ=+0.5mDa
[M+H-H2O-HF]+
RDB=11.0
296.1395
[C17H20N3O3]+
Δ=+0.3mDa
[M+H-HF]+
RDB=10.0
314.1500
[M+H]+
334.1561
Relative Abundance
m/z
D)
Metenr_3421 # 338 RT:4.31 AV:1 NL: 2.85E4
F: FTMS + p ESI Full ms2 342.10@hcd55.00 [50.00-1000.00]
[C13H13N2O]+
Δ=-0.7mDa
[M+H-CO2-C2H4-C3H7N]+
RDB=9.0
213.1021
227.1178
[C14H15N2O]+
Δ=-0.4mDa
[M+H-CO2-C2H4-C2H5N]+
RDB=9.0
[C15H14N3O2]+
Δ=+0.2mDa
[M+H-H2O-C2H4-C2H4]+
RDB=11.0
268.1081
[C18H24N3O]+
Δ=-0.6mDa
[M+H-CO2]+
RDB=9.0
298.1912
[C19H22N3O2]+
Δ=+0.1mDa
[M+H-H2O]+
RDB=11.0
324.1707
[M+H]+
342.1811
Relative Abundance
m/z
E)
metenr_3741 #374 RT:4.69 AV:1 NL:2.02E4
F: FTMS + p ESI Full ms2 374.10@hcd55.00 [50.00-1000.00]
[C14H13N2O3]+
Δ=-0.7mDa
[M+H-C2H4-C2H2N-H2CO2]+
RDB=10.0
257.0919
[C13H13N2O5]+
Δ=-0.7mDa
[M+H-C2H4-C4H7N]+
RDB=9.0
277.0817
[C15H13N2O4]+
Δ=-0.6mDa
[M+H-C2H4-C2H5N-H2O]+
RDB=11.0
285.0868
[C15H15N2O5]+
Δ=-1.5mDa
[M+H-C2H4-C2H5N]+
RDB=10.0
303.0971
[C18H24N3O3]+
Δ=-1.3mDa
[M+H-CO2]+
RDB=9.0
330.1970
[C19H22N3O4]+
Δ=-0.8mDa
[M+H-H2O]+
RDB=11.0
356.1602
[M+H]+
374.1707
Relative Abundance
m/z

Figure 5.